Mechanism and Free Energy of DNA Hybridization on Single-Walled Carbon Nanotubes Using Adaptive Biasing Force Simulations

Michael W. Chien[*], Robert R. Johnson[*], Shreekumar Pillai[*], Shree Ram Singh[**,***] and A. T. Charlie Johnson[*]

[*] Department of Physics and Astronomy and Nano/Bio Interface Center, University of Pennsylvania, Philadelphia, Pennsylvania 19104, USA, cjohnson@physics.upenn.edu
[**] Center for NanoBiotechnology Research, Alabama State University, Montgomery, Alabama USA

ABSTRACT

Vapor sensors based on functionalized carbon nanotubes (NTs) have shown great promise, with high sensitivity conferred by the reduced dimensionality and exceptional electronic properties of the NT. Critical challenges in the development of NT-based sensor arrays for electronic nose systems include the demonstration of reproducible fabrication methods and functionalization schemes that provide high chemical diversity to the resulting sensors. Here, we outline a scalable approach to fabricating arrays of vapor sensors consisting of NT field effect transistors functionalized with single-stranded DNA (DNA-NT). DNA-NT sensors were highly reproducible and target analytes were detected even in large backgrounds of volatile interferents. DNA-NT sensors were able to discriminate between highly similar molecules, including structural isomers and enantiomers. The sensors were also able to detect subtle variations in complex vapors, including mixtures of structural isomers and mixtures of many volatile organic compounds characteristic of humans. This work paves the way for incorporation of DNA-NT sensor arrays in "electronic nose"-type systems.

Keywords: carbon nanotube, DNA, hybridization

1 INTRODUCTION

DNA-carbon nanotube hybrids, consisting of single stranded DNA spontaneously adsorbed to the surface of single-walled carbon nanotubes (DNA-NT), have shown promise for use in sensitive and selective chemical vapor detection [1] and it has been proposed that this could be extended to the detection and sequencing of DNA [2]. Experiments have shown that DNA-NT hybrids suspended in solution are capable of detecting specific DNA sequences [3-5] and even resolving single nucleotide polymorphisms [6], with fluorescence [5,6] or electrochemical [3] readout. These findings must be reconciled with the expectation that strong attractive π-π stacking interactions between DNA bases and the NT sidewall [7,8,9] compete with the formation of hydrogen bonds between complementary DNA bases as required for Watson-Crick pairing (Fig. 1). The use of conventional molecular dynamics (MD) simulations to explore DNA hybridization in the presence of the NT is problematic due to the system's rugged potential energy landscape that can only be explored with long simulation times [9]. This motivated the use of adaptive biasing force (ABF) MD simulations [10], where a variable biasing force was applied to allow the system to overcome energy barriers. ABF simulations enabled the exploration of the possible reaction pathways that facilitate hybridization of DNA strands that were initially adsorbed to the NT. The hybridization of both GC and AT base pairs were investigated using short DNA strands. Analysis of many reaction pathways showed that significant conformational changes and complete desorption of DNA bases were required for DNA hybridization to occur. In order to estimate the free energy required for DNA hybridization, the potential of mean force (PMF) was calculated for a reaction pathway that started with DNA fully adsorbed to CNT and ended with DNA fully hybridized. The PMF (Figure 2) exhibits two distinct energy minima: a broad global minimum associated with DNA adsorbed to CNT and a narrower, higher energy minimum associated with fully hybridized DNA. The free energy differences between these two states were ~6 kcal/mol and ~10 kcal/mol for GC and AT base pairing, respectively. These values are consistent with GC base pairs having a stronger binding free energy due to the one additional hydrogen compared to AT base pairs. The PMF also showed that these two states are separated by a considerable energy barrier of ~5-10 kcal/mol. This result is in agreement with experiments that show that long equilibration timescales (~1 day) are needed to detect DNA hybridization using aqueous solutions of CNT. [5,6] These results further our understanding of DNA hybridization in the DNA-NT system, which is essential for the advancement of nanotechnology based on DNA-NT.

2 RESULTS AND DISCUSSION

ABF is uniquely suited to overcome the significant energy and conformational barriers preventing hybridization of DNA adsorbed onto NT [7,11], and enables estimates of the free energy change of hybridization by integration of the biasing force applied along the reaction coordinate [12] to generate the PMF for the system. The ABF method is computationally efficient [10]

and has been successfully applied to a variety of systems involving proteins, simple organic molecules, and other macromolecules dissolved in water and lipids [10,13].

All-atom ABF simulations were carried out using the NAMD 2.8 MD package [14] with a 2 fs timestep and a simulation box of size 3.9 nm x 3.9 nm x 6.9 nm, with three-dimensional periodic boundary conditions. Simulations were run at constant T = 300K and P= 1.013 bar using the Langevin piston method [15]. DNA and water were represented using the CHARMM22 force field [16] and TIP3P model [17], respectively. The NT atoms were modeled as uncharged Lennard-Jones particles with sp2 carbon parameters, as we did previously [7]. An (11,0) NT of length 50Å was centered in the box along the z-axis, and its atoms were restrained using a harmonic potential. Counter-ions (Na+) were added to balance the negatively charged DNA backbone. Electrostatic interactions were computed using the particle mesh Ewald method [18], and the van der Waals interactions were truncated with a 1.2 nm cutoff. Analysis and visualization of MD trajectories were performed with VMD [19].

ABF simulations were initialized with two complementary strands of ssDNA, each two bases long, with all four bases adsorbed to the (11,0) NT (Fig. 1), the minimum energy state as indicated by simulation [7,8,9,20] and experiment [11,20,21]. The first G-C base pair was initially hybridize, with hydrogen bonds reinforced by a harmonic potential to prevent separation, while the second base pair was initially un-hybridized. The ABF reaction coordinate was taken to be the distance between the central hydrogen-bonding sites of the second base pair, so ABF facilitated hybridization of the second base pair while the first base pair remained hybridized. There were no other constraints on the system; this reduced the likelihood of selection bias on the actual hybridization pathway. Unconstrained ABF simulations were conducted with a bin size of 10 pm, and 1000 samples per bin were used to determine the mean systemic force. In ABF simulation, hybridization occured rapidly (< 10 ns), while it was rarely observed on 100s of ns timescales in non-ABF MD. Twenty-three independent unconstrained ABF simulations were performed from identical initial coordinates to sample possible pathways to hybridization.

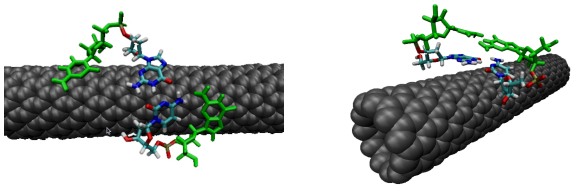

Figure 1. Initial and Final States of ABF MD Simulations. (left) Initial configuration of two GpC DNA strands with all bases adsorbed to the NT. The central GC base pair is hybridized, while the second base pair (green) is separated. (right) Final state of the system after ABF is conducted, and the second base pair is forced to hybridize. Based on analysis of ~20 reaction pathways, base desorption is necessary for the second base pair to form. Desorbed bases stack above the initial base pair, which remains adsorbed to the NT. The hybridized DNA structure is stable over ~100 ns timescales using conventional MD, which suggests that it is an energetically favorable configuration.

All pathways leading to hybridization of the two base pairs resulted in significant twisting of the DNA. In the dominant pathway (92% of cases), twisting was relieved when one base pair desorbed fully from the NT, and the base pairs hybridized in a Watson-Crick double helix with one base pair adsorbed to the NT and the other stacked above it (Fig. 1). MD Simulations of this state showed it to be meta-stable over tens of nanoseconds. Further constrained ABF simulations were run to better quantify the eneregetics of hybridization.

Constrained ABF was used to generate a PMF for the hybridization process. The simulations used a bin size of 0.5 pm and employed the root mean square displacement (RMSD) between the actual structure and a reference structure as the reaction coordinate. Sampling and updating of the biasing force was done as in unconstrained ABF simulations. To obtain more accurate quantitative results for the free energy barrier associated with hybridization, windowing was used to enforce even sampling of the system across the range of the reaction coordinate, from RMSD = 0.0 nm to approximately 0.8 nm. The reaction coordinate was divided into windows bounded by harmonic potentials, and the ABF simulation was initialized from a known conformation within the window derived from unconstrained ABF. Window size was varied according to the ruggedness of the energy landscape, from ca. 0.1 nm for reaction coordinate RMSD greater than 0.5 nm to ca. 0.025 nm for RMSD 0.05 – 0.3 nm.

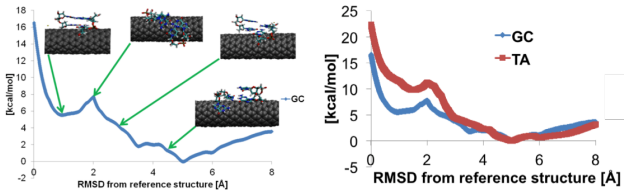

Figure 2. Potential of Mean force (PMF) for Different DNA Sequences. The PMF is a measure of the free energy change of a system along the reaction coordinate. (left) The PMF for hybridization of GpC-GpC exhibits a wide global minimum associated with both strands adsorbed to the NT and a smaller local minimum associated with hybridized DNA. (Insets) DNA conformations associated with the PMF, showing the reaction pathway leading to DNA hybridization. In order to hybridize, two of the bases desorb from the NT. (right) PMF for hybridization of GC and TA base pairs adjacent to an initially-hybridized GC pair. More energy is required to hybridize the TA base pair, due to differences in the DNA-stacking energies and the formation of fewer hydrogen bonds for TA.

The PMF derived from constrained ABF simulations was very rugged, as expected from the flexibility of the DNA-NT system [9], with two minima separated by a large energy barrier (Fig. 2). A local minimum near RMSD = 0.95 Å corresponded to the end state with both base pairs hybridized (RMSD differs from 0 due to imperfect energy minimization of the reference structure), while the minimum near RMSD = 5.0 Å corresponded to the initial state. Features of the PMF corresponded to specific conformations sampled by the system. The initial upward slope (RMSD ~ 4.4 Å) occured due to desorption of one base from the NT, and a second, steeper feature corresponded to desorption of the second base (RMSD ~ 3.0 Å). In the GCGC sequence, cytosine desorbed first with guanine following, in agreement with MD studies that found greater free energy of adsorption for guanine versus cytosine [7]. The PMF contained an energy barrier at RMSD ~ 2.0 Å with a height of +7.7 kcal/mol with contributions from (1) breaking of π-π stacking between DNA bases and the NT, (2) solvation of DNA in water, (3) solvation of NT previously covered byDNA [7], and (4) entropic effects from forming the double helix. The decrease in potential energy of 2.2 kcal/mol to the local minimum at RMSD = 0.95Å corresponds to hybridization of the second base pair, with energy lowering from Watson-Crick hydrogen bonding and DNA stacking interactions. The overall free energy change of the reaction, from initial adsorbed to final hybridized state, is ΔF = +5.54 kcal/mol (Fig. 2 and Table 1).

Similar results were obtained for ABF simulations performed for GT-CA hybridization (Fig. 2). The PMF for the hybridization of the TA base pair had a similar structure, with two regions of different slopes corresponding to desorption and stacking of thymine, in this case, followed by adenine. The energy barrier (RMSD ~ 2.0 Å) was found to be +11.17 kcal/mol and the overall free energy change of hybridization was ΔF = +9.78 kcal/mol. The fact that more energy is required to hybridize the TA base pair versus the GC base pair was ascribed to two factors: 1) although it was showed in a previous study that the energy required to desorb a GC pair from a NT is nearly identical to an TA pair, hybridization of a GC base pair is energetically favored due to the formation of three hydrogen bonds compared to two for an AT pair; and 2) energy differences resulting from different DNA-DNA stacking interactions for the two cases.

It is important to note that these energy estimates are based upon sampling of a single, dominant pathway resulting in hybridization of two adjacent base pairs. This pathway, which results in desorption of one base pair to form a double helix, was favored pathway in the unconstrained ABF simulations, occurring in 92% of hybridization events. However, a small percentage of hybridization events result from alternate pathways with different conformations and energy changes. The effect of these alternate pathways on the PMF of the system will be explored in the future.

3 CONCLUSION

The ABF simulations conducted here led us to conclude that hybridization of complementary DNA adsorbed on NT is significantly hindered. Hybridization of single base pairs at random is possible, but there are significant energy barriers preventing hybridization of adjacent base pairs due to the need for base desorption. Hybridization of multiple adjacent base pairs, as necessary for the complete or partial respectively, at room temperature (Table 1). The energy required to hybridize longer DNA sequences would be correspondingly higher. Factors not considered here include the possibility that large quantities of DNA crowd the NT hybridization of long DNA sequences, would be expected to incur significant energy penalties. Free energy changes required for hybridization of GC or TA adjacent to an already-hybridized GC are 9.7 k_BT and 17.1 k_BT, surface, facilitating desorption of some bases. Combined with long equilibration times typical of some experiments [5,22], it is conceivable that the energy barriers could be overcome, leading to partial hybridization of longer DNA sequences and formation of a characteristic average number of base pairs, depending on the DNA sequence and experimental conditions. The introduction of a single nucleotide polymorphism could cause a slight change in the average number of base pairs formed, leading to the slight fluorescent signal shifts observed in these experiments [22].

This work was supported by the Nano/Bio Interface Center (NSF NSEC DMR 08-32802) and NSF-CREST (HRD 07-34232) and NSF-HBCU-UP (HRD 05-05872).

Table 1. Free Energy Changes and Energy Barriers for GC and TA Base Pairing. The free energy change (ΔF) is defined as the energy difference between the global minimum of the PMF (Figure 2) and the local minimum associated with fully hybridized DNA The barrier height is the energy difference between the global minimum of the PMF and the energy maximum at RMSD ~ 2Å.

	ΔF [kcal/mol]	ΔF [k_BT] at 300K	Barrier [kcal/mol]	Barrier [k_BT] at 300K
G-C	**5.54**	**9.7**	**7.74**	**13.6**
T-A	**9.78**	**17.1**	**11.17**	**19.6**

4 REFERENCES

[1] S.M. Khamis, R.A. Jones, A. T. C. Johnson, G. Preti, J. Kwak, and A. Gelperin, AIP Advances **2**, 022110 (2012).

[2] S. Meng, W. L. Wang, P. Maragakis, and E. Kaxiras, Nano Lett. **7** (8), 2312 (2007).

[3] J.E. Weber, S. Pillai, M. K. Ram, A. Kumar, and S.R. Singh, Mater. Sci. Eng., C **31**, 821 (2011).

[4] A. Star, E. Tu, J. Niemann, J. C. P. Gabriel, C.S. Joiner, and C. Valcke, Proc. Natl. Acad. Sci. U. S. A. **103**, 921 (2006).

[5] E. S. Jeng, A. E. Moll, A. C. Roy, J. B. Gastala, and M. S. Strano, Nano Lett. **6** (3), 371 (2006).

[6] E. S. Jeng, J.D. Nelson, K.L.J. Prather, and M. S. Strano, Small **6**, 40 (2010).

[7] Robert R. Johnson, A. T. Charlie Johnson, and Michael L. Klein, Small **6** (1), 31 (2010).

[8] R. R. Johnson, A. T. C. Johnson, and M. L. Klein, Nano Lett. **8** (1), 69 (2008); M. Zheng, A. Jagota, E. D. Semke, B. A. Diner, R. S. Mclean, S. R. Lustig, R. E. Richardson, and N. G. Tassi, Nat Mater **2** (5), 338 (2003); H. J. Gao and Y. Kong, Ann. Rev. Mater. Res. **34**, 123 (2004).

[9] Robert R. Johnson, Axel Kohlmeyer, A. T. Charlie Johnson, and Michael L. Klein, Nano Lett. **9** (2), 537 (2009).

[10] J. Henin and C. Chipot, J. Chem. Phys. **121** (7), 2904 (2004).

[11] F. Albertorio, M. E. Hughes, J. A. Golovchenko, and D. Branton, Nanotechnology **20** (39) (2009).

[12] E. Darve and A. Pohorille, J. Chem. Phys. **115** (20), 9169 (2001).

[13] W. S. Cai, T. T. Sun, P. Liu, C. Chipot, and X. G. Shao, J. Phys. Chem. B **113** (22), 7836 (2009); C. Y. Wei and A. Pohorille, J. Am. Chem. Soc. **131** (29), 10237 (2009); D. Rodriguez-Gomez, E. Darve, and A. Pohorille, J. Chem. Phys. **120** (8), 3563 (2004).

[14] J. C. Phillips, R. Braun, W. Wang, J. Gumbart, E. Tajkhorshid, E. Villa, C. Chipot, R. D. Skeel, L. Kale, and K. Schulten, J. Comput. Chem. **26** (16), 1781 (2005).

[15] S. E. Feller, Y. H. Zhang, R. W. Pastor, and B. R. Brooks, J. Chem. Phys. **103** (11), 4613 (1995).

[16] A. D. Mackerell, M. Feig, and C. L. Brooks, J. Comput. Chem. **25** (11), 1400 (2004).

[17] W. L. Jorgensen, J. Am. Chem. Soc. **103** (2), 335 (1981).

[18] T. Darden, D. York, and L. Pedersen, J. Chem. Phys. **98** (12), 10089 (1993).

[19] W. Humphrey, A. Dalke, and K. Schulten, J. Mol. Graph. **14** (1), 33 (1996).

[20] S. Meng, P. Maragakis, C. Papaloukas, and E. Kaxiras, Nano Lett. **7** (1), 45 (2007).

[21] M. Zheng, A. Jagota, M. S. Strano, A. P. Santos, P. Barone, S. G. Chou, B. A. Diner, M. S. Dresselhaus, R. S. McLean, G. B. Onoa, G. G. Samsonidze, E. D. Semke, M. Usrey, and D. J. Walls, Science **302** (5650), 1545 (2003).

[22] E. S. Jeng, J. D. Nelson, K. L. J. Prather, and M. S. Strano, Small **6** (1), 40 (2010).